Wiley Online Library
Early View publication on www.wileyonlinelibrary.com
(issue and page numbers not yet assigned;
citable using Digital Object Identifier – **DOI**)

Phys. Status Solidi B, 1–5 (2016) / **DOI** 10.1002/pssb.201600631

physica status solidi b
www.pss-b.com
basic solid state physics

Pulsed electron-nuclear double resonance diagnostics of Ce^{3+} emitters in scintillating garnets

A. G. Badalyan[*,1], G. V. Mamin[2], Yu. A. Uspenskaya[1], E. V. Edinach[1], H. R. Asatryan[1], N. G. Romanov[1], S. B. Orlinskii[2], P. G. Baranov[1,3], V. M. Khanin[3,4], H. Wieczorek[4], and C. Ronda[4]

[1] Ioffe Institute, 194021 St. Petersburg, Russia
[2] Kazan Federal University, Institute of Physics, 18 Kremlyovskaya str., 420008 Kazan, Russia
[3] Peter the Great St. Petersburg Polytechnic University, 195251 St. Petersburg, Russia
[4] Philips Research, High Tech Campus 4, 5656 AE Eindhoven, The Netherlands

Received 22 September 2016, revised 18 November 2016, accepted 29 November 2016
Published online 19 December 2016

Keywords ceramics, cerium, emitters, garnets, pulsed electron-nuclear double resonance, pulsed electron paramagnetic resonance

[*] Corresponding author: e-mail andrey.badalyan@mail.ioffe.ru, Phone: +7 812 2927320, Fax: +7 812 2971017

Pulsed electron paramagnetic resonance (EPR) and pulsed electron-nuclear double resonance (ENDOR) techniques have been applied to study the environment of luminescent Ce^{3+} ions in garnet based scintillator powders and ceramics. The presence of aluminum and gallium isotopes with large nuclear magnetic and quadrupole moments in the nearest neighborhood of the Ce^{3+} ion allows for the use of the hyperfine and quadrupole interactions with these ions for determination of the unpaired electron spatial distribution and the definition of the electric field gradient at the aluminum and gallium sites. Pulsed EPR and ENDOR techniques made it possible to study the coherent properties of the Ce^{3+} spin system in garnet powders and ceramics, which is important for spin manipulation on Ce^{3+} centers.

1 Introduction Garnet single crystals and ceramics doped with cerium are widely used as scintillator materials that convert high energy radiation into visible or infrared light [1]. Yttrium aluminum garnet (YAG) doped with cerium is a key component in light emitting diodes (LEDs) and lasers [2]. The phosphor absorbs part of the blue light emitted by an (In,Ga)N LED and converts it into yellow emission, which together with partly transmitted blue light yields white light.

Recently coherent properties of rare-earth single-spin qubits in YAG have been demonstrated [3, 4]. It was declared that rare-earth-doped crystals are excellent hardware for quantum storage of optical information. Combined with the high brightness of Ce^{3+} emission and the possibility of creating photonic circuits out of the host material, this makes cerium spins an interesting option for integrated quantum photonics.

Ce^{3+} has only one 4f electron and therefore, presents the simplest example of 5d–4f emission. The ground state $4f^1$ configuration of Ce^{3+} yields two levels, $^2F_{5/2}$ and $^2F_{7/2}$, separated by approximately 2000 cm^{-1} as a result of spin–orbit coupling so that one can observe the 5d–4f emission bands separated into two distinct peaks, especially at low Ce^{3+} concentrations, lower than a few mole percent. In the host lattice, 5d orbitals of Ce^{3+} participate in chemical bonding and thus a strong influence of the surroundings on 5d level splitting and spectral position is observed.

Garnets crystallize in a cubic form and are described by the formula $C_3A_2D_3O_{12}$, (which can be commonly written as $C_3(A,D)_5O_{12}$), where three different cation sites are indicated. C is a dodecahedral site, A and D are an octahedral and a tetrahedral sites, respectively. The site C can be occupied by Y or Lu (diamagnetic state). In these materials, sites A and D are occupied by aluminum but can also be substituted by other elements, for example gallium.

The emission efficiency depends on the position of the Ce^{3+} ion in the garnet crystal lattice and its environment, including the presence of defects in its immediate vicinity. In a number of publications the optical properties of an yttrium gallium aluminum garnet, $Y_3(Ga,Al)_5O_{12}$, and a lutetium gallium aluminum garnet, $Lu_3(Ga,Al)_5O_{12}$, doped with Ce^{3+} were investigated as a function of the Ga/Al ratio,

aiming at understanding the influence of replacing Al^{3+} by Ga^{3+} on the optical properties of these materials. The literature is not conclusive on the sequence which sites Ga first replaces Al, either the octahedral or the tetrahedral sites [5–7]. The two sites have different properties, as we show in this article where pulsed electron paramagnetic resonance (EPR) and electron-nuclear double resonance (ENDOR) techniques are used in diagnosing the cerium environment in garnet powders and ceramics.

2 Experimental All $Lu_3Al_5O_{12}$ and $Y_3(Ga,Al)_5O_{12}$ ceramic samples were prepared at Philips Research Eindhoven by sintering of oxide raw materials. Based on X-ray diffraction patterns it was concluded that all samples consist of a single garnet phase. They were doped with cerium in concentration 0.2%. The X-band electron spin echo (ESE) detected EPR spectra were measured by using the Hahn-echo decay sequence $\pi/2-\tau-\pi$, with $\pi/2=16$ ns and $\tau=180$ ns. To measure T_2 the ESE signal amplitude was monitored by using the Hahn-echo decay sequence $\pi/2-\tau-\pi$, where τ was varied from 180 ns up to 2.2 μs, $\pi/2=16$ ns. ENDOR was measured by using Mims sequence $\pi/2-\tau-\pi/2-T-\pi/2-\tau-$ESE, $\tau=228$ ns, $T=19.8$ μs, for RF pulse $T_{RF}=18$ μs.

3 Results and discussion The EPR spectra of Ce^{3+} ions can be described by a simple spin Hamiltonian taking into account the Zeeman interaction for a paramagnetic center with the effective spin $S=1/2$ and an anisotropic g-factor that greatly depends on the composition of the garnet crystal (C–Y, Lu, rare-earth element; A and D – Al or Ga). EPR allows us to get detailed information about the g-factors, but generally it is not possible to obtain information about the hyperfine interactions with the surrounding magnetic nuclei, as well as to explore the quadrupole interactions. ENDOR is the method of choice for these purposes.

Figure 1 shows the X-band (9.4 GHz) ESE detected EPR signal of Ce^{3+} ions in $Lu_3Al_5O_{12}$:Ce (0.2% Ce) ceramics. An asymmetric EPR line shape is due to the fact that the number of spin packets contributing to the spectrum is much larger in the xy-plane than along the z-axis. This line shape can be simulated, assuming a large number of paramagnetic centers with random orientation with respect to the static magnetic field. For a given magnetic field strength B_0, all spins fulfilling the resonance condition $B_0=h\nu/[g(\theta)\mu_B]$, that is all spins for which B_0 makes an angle θ with the z-axis, contribute to the spectrum and are considered to form a spin packet. The extreme positions of the spectrum are obtained by inserting g_x, g_y, and g_z into the resonance condition. It should be noted that for g_x, $g_y > g_z$, one obtains $B_0(g_x,g_y) < B_0(g_z)$ due to the inverse proportionality of g and B_0. Simulation of continuous wave (cw) EPR spectra in powder samples can be done relatively easily since the signal intensity is proportional to the number of centers in the selected volume. In this study, EPR spectra were detected using two-pulse spin echo at a fixed delay

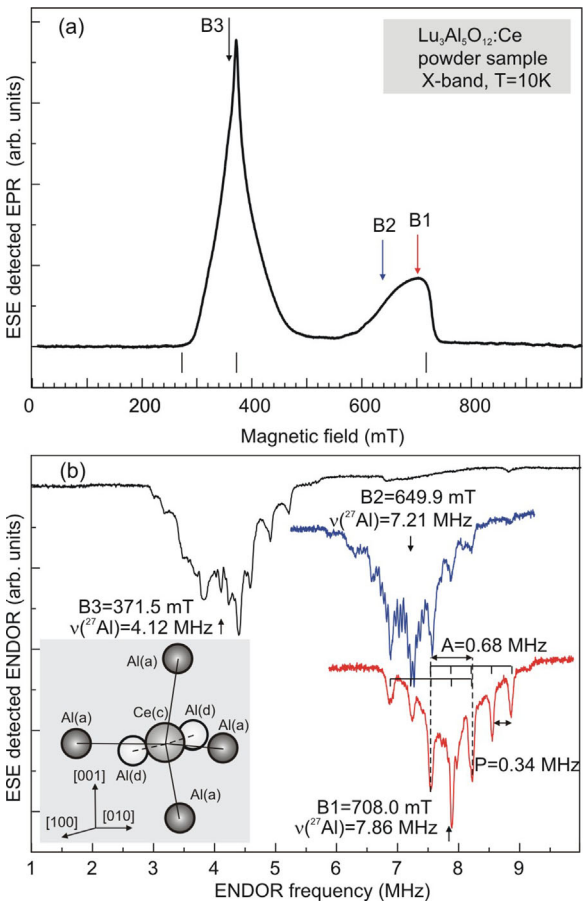

Figure 1 ESE detected EPR (a) and ENDOR (b) signals of Ce^{3+} ions in $Lu_3Al_5O_{12}$:Ce ceramic sample. The inset in (b) shows a sketch of the nearest environment of the Ce^{3+} ion with aluminum atoms in two positions A and D; the distances between the Ce^{3+} ion and aluminum atoms in the nearest octahedral and tetrahedral positions are 3.33 and 2.98 Å, respectively.

time τ between the pulses. In this case, variations of τ result in modulation effects, which are caused by surrounding nuclei and will be discussed below. The modulation period is close to the period of nuclear precession that depends on the magnetic field strength, so the measured ESE signal can fall at different points of the modulation curve corresponding to its maximum, minimum, or in between. This complicates very much analysis of the shape of ESE-detected EPR spectra. In addition, such a simulation is challenging since the relaxation times depend on the orientation of a center in magnetic field and the magnetic field magnitude. In Fig. 1(a) we have marked by bars the positions of lines with g-factor principal values for Ce^{3+} in $Lu_3Al_5O_{12}$ single crystals measured in Ref. [8]: $g_x=2.614$, $g_y=1.865$, $g_z=0.961$. It is evident that these positions do not always correspond to the ESE detected EPR spectra.

The ENDOR spectra were measured at magnetic fields marked in Fig. 1(a) as B1, B2, and B3: B1 = 708.0 mT, B2 = 649.9 mT, and B3 = 371.5 mT. Figure 1(b) shows the groups of lines arranged symmetrically with respect to the

^{27}Al nuclear Zeeman frequencies $\nu(^{27}\mathrm{Al})$ indicated by arrows. These groups are related to the hyperfine (HF) and quadrupole interactions with the neighboring aluminum atoms. To analyze the Ce^{3+} EPR and ENDOR spectra the following spin Hamiltonian with $S = 1/2$ has been used:

$$\hat{H} = \mu_B \vec{B} \cdot \hat{g} \cdot \hat{\vec{S}} + \sum_i (\hat{\vec{S}} \cdot \hat{A}_i \cdot \hat{\vec{I}}_i + \hat{\vec{I}}_i \cdot \hat{P}_i \cdot \hat{\vec{I}}_i - g_N \mu_N \vec{B} \cdot \hat{\vec{I}}_i), \quad (1)$$

where $\hat{\vec{S}}$ is the electron spin operator, $\hat{\vec{I}}_i$ is the nuclear spin operator for the i- nucleus of aluminum (gallium), which are summed over the aluminum (gallium) nuclei that interact with the electron. The $\hat{g}$-tensor reflects the symmetry around the Ce^{3+} ion. The first term describes the electron Zeeman interaction, the following terms in Eq. (1) describe the HF, quadrupole, and nuclear Zeeman interactions with ligand ions, respectively (cerium has only even isotopes ^{140}Ce, ^{142}Ce with nuclear spin $I = 0$). Here g_N is the g-factor of the aluminum (gallium) nucleus, and μ_B and μ_N are the Bohr magneton and nuclear magneton, respectively.

The HF interaction parameters can be described in terms of the isotropic part a, and anisotropic parts b and b', which are related to the principal HF tensor coordinates (xyz): $A_{xx} = a - b + b'$, $A_{yy} = a - b - b'$, $A_{zz} = a + 2b$. The diagonal matrix elements of the nuclear quadrupole interaction in the principal coordinates are $P_{xx} = -q + q'$, $P_{yy} = q - q'$, $P_{zz} = 2q$. Here, b' and q' denote the deviation from the axial symmetry that we neglect in this analysis ($b' = 0$, $q' = 0$). In case of the axial symmetry the term in Eq. (1), which describes the quadrupole interaction of the aluminum or gallium nuclei, can be written as $H_Q = P[I_z^2 - 1/3I(I+1)]$, here $P = 3/2P_{zz} = 3q$ [9].

The isotropic component of the HF interaction reflects the spin density of the s-electron wave function at the site of the nucleus and the anisotropic component reflects the spin density of the p-electron wave function. For the paramagnetic center with $S = 1/2$ the related ENDOR transition frequencies for interaction with the i-nucleus of aluminum (gallium) [9]

$$\nu_i = 1/h \left| g_N \mu_N B_0 \pm \frac{1}{2}[a_i + b_i(3\cos^2\theta - 1)] \right| + 3m_q q_i(3\cos^2\theta - 1), \quad (2)$$

where B_0 is the magnetic field corresponding to the EPR resonance conditions. Each nucleus gives rise to ENDOR transitions symmetrically placed around its nuclear Zeeman frequency $\nu_Z = 1/h(g_N \mu_N B_0)$ in the high magnetic field approximation. The "+" and "−" signs in the equation denote the ENDOR lines for $M_S = +1/2$ and $M_S = -1/2$, respectively.

For the nuclear spin $I > 1/2$ (Al, Ga) the quadrupole interaction of the nucleus with an electric field gradient must be taken into account by $q_i = (eQ_0)/[4I(2I-1)]V_{zz}(r_i)$. Here Q_0 is the electric quadrupole moment of Al (Ga) in multiples of $|e| \times 10^{-24}\,\mathrm{cm}^2$, $V_{zz}(r_i)$ is the electrical field gradient, and $m_q = [m_I + (m_I + 1)]/2$ is the average value of the nuclear quantum states m_I between which the nuclear transition takes place. For ^{27}Al the nuclear spin is $I = 5/2$, giving five m_q-values: ±2, ±1, and 0. Thus, the quintet in Fig. 1(b) is due to the quadrupole interaction of ^{27}Al. Natural abundance of ^{27}Al is 100%, the nuclear g-factor $g_N = 1.4566$, and the electric quadrupole moment $Q = 0.15$ (Appendix A in [9]).

To the best of our knowledge, the values of the HF and quadrupole interactions with aluminum nuclei were not known prior to this work since these interactions are not resolved by EPR.

The value of the isotropic HF interaction ($A = 0.68$ MHz) allows for estimating the spin density of the s-electron on the aluminum nuclei. The wave function for the unpaired electron can be approximated by a linear combination of atomic orbitals centered on the aluminum atoms near the Ce^{3+} ion as $\psi = \alpha\psi_{3s} + \beta\psi_{3p}$, $\alpha^2 + \beta^2 = 1$. One can only make some assumptions about the anisotropic part of the interaction. Assuming sp^3-hybridization, which is the most realistic in this case, 25% of the spin density is on the s-orbital, and with 75% of the spin density on the p-orbital. In this case, the total spin density is about four times larger than the measured value for the unpaired s-electron, that is about 0.1% of that for free Al atom. We used data from Ref. [10], where the isotropic HF interaction constant for 3s wave function of free Al atom is ∼3911 MHz and the anisotropic HF interaction constant for 3p wave function is about 20 times smaller.

The quadrupole splitting depends on the orientation of the magnetic field relative to the direction of the electric-field gradient. The magnitude of this splitting between the neighboring lines varies from P for the perpendicular orientation of the magnetic field to $2P$ for the parallel orientation, passing through zero at an angle of about 55°. Furthermore, we must consider the complex combination of the HF and quadrupole interactions, which also depend on orientation. The most probable orientation of the center in a powder or ceramic sample is the perpendicular orientation since the number of centers contributing to the spectrum is much larger in the perpendicular plane than along the parallel axis, and therefore the splitting between the most intense neighboring lines will be considered as P, the HF interaction being considered as isotropic. Of course, to obtain more accurate information about the parameters of the spin Hamiltonian (1) one should use single crystals and study the orientation dependence of EPR and ENDOR spectra, which is an extremely time-consuming work. The advantage of powder and ceramic samples is the fact that the nature itself produces an average over all orientations and highlights the main parameters of the EPR and ENDOR spectra.

The above statements are only valid for powder spectra of centers with an isotropic g-factor. In our description, we proceed from the fact that in each case we choose not the entire spectrum, but only a part of it with a limited range of the g-factor variations. That is, in each case we deal with a

quasi-isotropic behavior of g-factor. We plan to expand the range of research facilities (more magnetic field points in ESE-detected EPR spectra, more samples including single crystals) and make more detailed calculations. It should be mentioned that ENDOR signals were not observed in the cw EPR experiments.

Resolved nuclear quadrupole splitting allows for the direct determination of the electric field gradient at the nuclear position. Usually two sources of the electric field gradient $V_{zz}(r_i)$ are considered: intrinsic electric-field gradients in different crystal lattice positions, which are due to the crystal structure of a garnet, and the unpaired charge density in the np orbital (3p-orbital of the ^{27}Al ion). From the anisotropic part of the HF interaction, the magnitude of the latter was estimated to be very small, thus we can estimate the contribution of the garnet electric field gradient. The quadrupole splitting, caused by ^{27}Al nuclei surrounding the Ce^{3+} ion, is $P \cong 0.34$ MHz, and the electric field gradient $V_{zz}(\mathrm{Al}) = 1.25 \times 10^{21}$ V/m^2.

In Fig. 1(b) there are at least two types of ENDOR spectra for aluminum, differing in magnitude of the quadrupole interaction. It is known that aluminum can occupy two positions in the garnet crystal lattice ($C_3A_2D_3O_{12}$), an octahedral position (a) and a tetrahedral one (d). Since the electric field gradients can be different in these positions, the quadrupole splitting for ^{27}Al nuclei should be different. We assume that the large and small splitting match the aluminum ions occupying one of the two possible positions. To identify the position, it is necessary to know the electric field gradients at various positions in aluminum garnet and for this purpose, the NMR data or theoretical calculations can be used. Calculated and measured values of the electric field gradient at aluminum sites in various garnets are presented in [11]. It was shown that the electric field gradient in a tetrahedral position (d) is several times greater that in an octahedral site (a). Thus, we can assume that the spectra with a large quadrupole splitting are consistent with HF interaction with Al ions occupying a tetrahedral positions (d), whereas spectra with small quadrupole splitting belong to Al in octahedral position (a). As a result the ENDOR data can be used in mixed garnets for studying the replacement process.

Figure 2 shows ESE detected EPR (a) and ENDOR (b) signals of Ce^{3+} ions in a $Y_3Ga_2Al_3O_{12}$:Ce ceramic sample. The magnetic fields B1 = 655.0 mT and B2 = 335.2 mT correspond to the values at which ENDOR measurements were performed. The positions of the line with the g-factor principal values measured for $Y_3Ga_5O_{12}$:Ce single crystals ($g_x = 2.00$, $g_y = 1.63$, $g_z = 0.85$ [12]) are shown in Fig. 2(a) by bars. The inset in (b) presents the central part of the ENDOR spectrum for B1 = 655.0 mT in enlarged scale. The central part of the ENDOR spectrum of $Lu_3Al_5O_{12}$:Ce for B2 = 649.9 mT from Fig. 1(b) is shown by dashed line for comparison. The arrows mark the ^{27}Al Zeeman frequency. It can be seen that the splitting between the neighboring lines is practically the same and is approximately equal to 0.05 MHz.

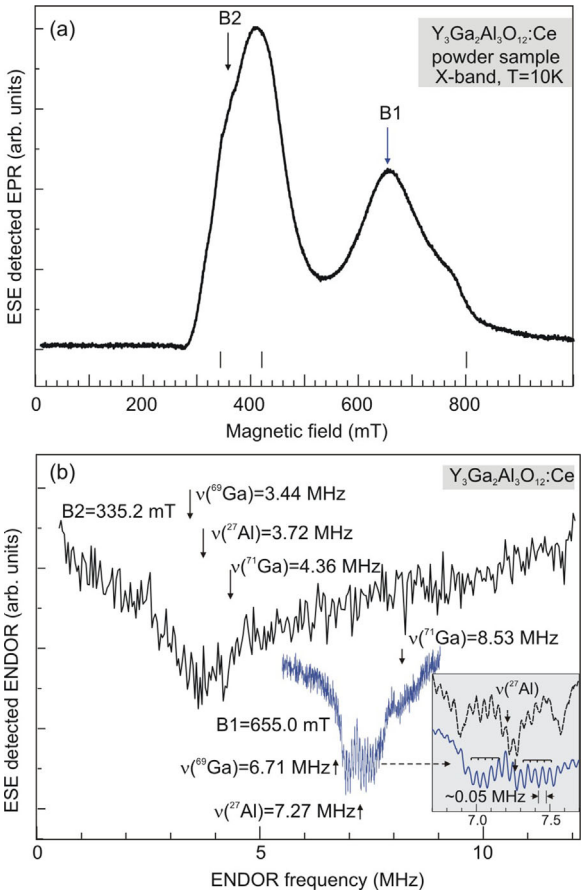

Figure 2 (a) ESE detected EPR signal of Ce^{3+} ions in a $Y_3Ga_2Al_3O_{12}$:Ce ceramic sample. (b) ESE detected ENDOR signal of Ce^{3+} ions in $Y_3Ga_2Al_3O_{12}$:Ce ceramic sample. The inset shows the enlarged central part of the ENDOR spectra for B1, the central part of the ENDOR spectrum of $Lu_3Al_5O_{12}$:Ce for $B = 649.9$ mT from Fig. 1(b) is shown by dashed line for comparison.

We assume that this splitting is the quadrupole splitting for aluminum occupying an octahedral position (a) with a smaller electric field gradient. Thus, $P \approx 0.05$ MHz and the electric field gradient $V_{zz}(\mathrm{Al}) \approx 1.8 \times 10^{20}$ V/m^2. To explain the presence of a larger number of lines than one can expect for the HF interaction only, we assume that there is an interaction with different HF constants A ≈ 0, 0.35, 0.65 MHz due to a combination of several local environments. Naturally, the HF and quadrupole interactions with each type of aluminum atoms can be different, as it is indeed observed in the experiment. There are several possible configurations of the Ce^{3+} ion nearest environment, so in the experiment we observe an average picture. The HF interaction with Al neighbors is suggested to be transferred through the oxygen ligands that surround cerium and aluminum.

In contrast to aluminum, no structure has been resolved for gallium nuclei. There are two isotopes of gallium: ^{69}Ga, $I = 3/2$, 60.1%, $g_N = 1.3444$, $Q = 0.168$ and ^{71}Ga, $I = 3/2$,

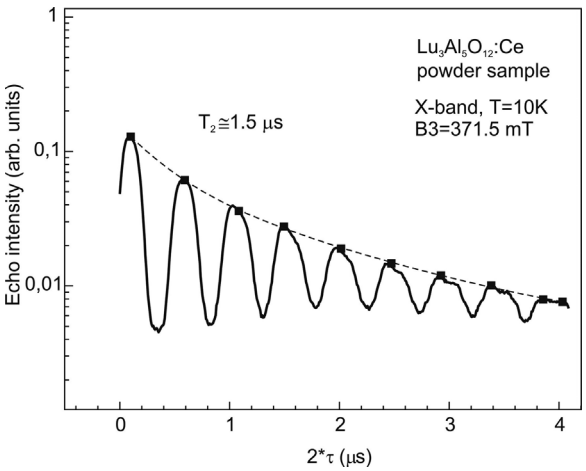

Figure 3 Decay process of the transverse magnetization of $Lu_3Al_5O_{12}$:Ce ceramics. Visible oscillations are caused by the Larmor precession of the magnetic moments of the surrounding nuclei.

39.9%, $g_N = 1.7082$, $Q = 0.106$ (Appendix A in [9]). The values of the gallium quadrupole moments are close to that for ^{27}Al, so one can suppose comparable values of the quadrupole splitting. However, the HF interaction for Ga isotopes will be at least several times larger as compared to ^{27}Al.

The table from [10] shows that the isotropic ^{69}Ga central-atom HF interaction constant for 4s-electron is 12,210 MHz (15,515 MHz for ^{71}Ga), more than three times larger compared to that for ^{27}Al. Therefore, this will lead to a substantial broadening of the lines by averaging of the powder spectra, which in turn causes the lack of a resolved structure.

Coherent spin properties of the rare-earth Ce^{3+} emitters in garnet powder and ceramic have been demonstrated in this work. To measure T_2 the ESE signal amplitude was monitored by using the Hahn-echo decay sequence $\pi/2 - \tau - \pi$, and τ was varied from 180 ns up to 2.2 μs, $\pi/2 = 16$ ns. Figure 3 shows the decay process of the transverse magnetization of $Lu_3Al_5O_{12}$:Ce ceramics. Visible oscillations are caused by the Larmor precession of the magnetic moments of the surrounding nuclei. These measurements can be used as an indicator of the presence of a number of nuclei. The HF interaction with aluminum nuclear spins combined with the high brightness of Ce^{3+} emission can be exploited as an interface between photons and long-lived nuclear spin memory [3, 4].

There is a relaxation process with $T_2 = 1.5$ μs. The estimated T_1 value is of the order of 20 μs at 10 K.

4 Summary In conclusion, EPR and ENDOR techniques were applied to measure hyperfine and quadrupole interactions for Ce^{3+} in garnet based scintillator powders and ceramics for assessment of the unpaired electron spatial distribution and definition of the electric field gradient at aluminum and gallium sites. The Ce^{3+} g-factor anisotropy can be used in ENDOR experiment for diagnostic of the cerium environment in mixed garnet ceramics, to distinguish between aluminum and gallium in the nearest neighborhood of Ce^{3+}. First results were obtained on the quadrupole interaction for aluminum nuclei in garnet ceramics, and octahedral and tetrahedral Al positions were separated. Pulsed EPR and ENDOR techniques enable determining the coherence of the Ce^{3+}spin system. We are planning to expand the range of research facilities (more magnetic field points in ESE-detected EPR spectra, more samples including single crystals) and make more detailed calculations. In this report we would like only to show that pulsed ESE-ENDOR methods open up wide opportunities for the research and diagnosis of disordered garnet crystal systems.

Acknowledgements This work has been supported by the Russian Science Foundation under Agreement No. 14-12-00859 and by Philips.

References

[1] H. Ogino, A. Yoshikawa, M. Nikl, J. A. Mares, J. Shimoyama, and K. Kishio, J. Cryst. Growth **311**, 908 (2009).
[2] V. Bachmann, C. R. Ronda, and A. Meijerink, Chem. Mater. **21**, 2077 (2009).
[3] P. Siyushev, K. Xia, R. Reuter, M. Jamali, N. Zhao, N. Yang, C. Duan, N. Kukharchyk, A. D. Wieck, R. Kolesov, and J. Wrachtrup, Nature Commun. **5**, 3895 (2014).
[4] R. Kolesov, K. Xia, R. Reuter, M. Jamali, R. Stohr, T. Inal, P. Siyushev, and J. Wrachtrup, Phys. Rev. Lett. **111**, 120502 (2013).
[5] A. B. Muñoz-García and L. Seijo, Phys. Rev. B **82**, 184118 (2010).
[6] C. R. Stanek, C. Jiang, S. K. Yadav, K. J. McClellan, B. P. Uberuaga, D. A. Andersson, and M. Nikl, Phys. Status Solidi B **250**, 244 (2013).
[7] A. Nakatsuka, A. Yoshiasa, and T. Yamanaka, Acta Crystallogr. B **55**, 266 (1999).
[8] A. Vedda, M. Martini, D. Di Martino, V. V. Laguta, M. Nikl, E. Mihokova, J. Rosa, K. Nejezchleb, and K. Blazek, Radiat. Eff. Defects Solids **157**, 1003 (2002).
[9] J.-M. Spaeth, J. R. Niklas, and R. H. Bartram, Structural Analysis of Points Defects in Solids (Springer-Verlag, Berlin, Heidelberg, 1992).
[10] J. R. Morton and K. F. Preston, J. Magn. Reson. **30**, 577 (1978).
[11] V. H. Schmidt and E. D. Jones, Phys. Rev. B. **1**, 1978 (1970).
[12] R. L. White, T. G. Phillips, and R. A. Lefever, J. Appl. Phys. **38**, 408 (1967).